Journal of the Korean Society of Surveying, Geodesy, Photogrammetry and Cartography
Vol. 34, No. 4, 373-382, 2016
http://dx.doi.org/10.7848/ksgpc.2016.34.4.373
ISSN 1598-4850(Print)
ISSN 2288-260X(Online)
Original article

Analysis of Database Referenced Navigation by the Combination of Heterogeneous Geophysical Data and Algorithms

Lee, Jisun[1)] · Kwon, Jay Hyoun[2)]

Abstract

In this study, an EKF (Extended Kalman Filter) based database reference navigation using both gravity gradient and terrain data was performed to complement the weakness of using only one type of geophysical DB (Database). Furthermore, a new algorithm which combines the EKF and profile matching was developed to improve the stability and accuracy of the positioning. On the basis of simulations, it was found that the overall navigation performance was improved by the combination of geophysical DBs except the two trajectories in which the divergence of TRN (Terrain Referenced Navigation) occurred. To solve the divergence problem, the profile matching algorithm using the terrain data is combined with the EKF. The results show that all trajectories generate the stable performance with positioning error ranges between 14m to 23m although not all trajectories positioning accuracy is improved. The average positioning error from the combined algorithm for all nine trajectories is about 18 m. For further study, a development of a switching geophysical DB or algorithm between the EKF and the profile matching to improve the navigation performance is suggested.

Keywords : GGTRN, Profile Matching, Heterogeneous DB and Algorithm, Combination of DB and Algorithm

1. Introduction

An alternative navigation system which compensates INS (Inertial Navigation System) error based on the geophysical DB (Database) has been studied to determine the position of a moving vehicle under non-GNSS (Global Navigation Satellite System) environments such as GNSS signal jamming or solar storms. Among various geophysical DBRN (Database Referenced Navigation) systems, TRN (Terrain Referenced Navigation) is the most popular, and it already has been adopted for the airplane or missile navigation (Hollowell, 1990; Laur and Llanso, 1995; Cowie *et al*., 2008; Wang and Bian, 2008). Recently, some studies show interests in the GGRN (Gravity Gradient Referenced Navigation) as a rising technique for the submarine navigation on the strength of development of precise sensor (Zhang *et al*., 2004; Richeson, 2008; Rogers, 2009; Liu *et al*., 2010; DeGregoria, 2010). In DBRN, various navigation algorithms (e.g. profile matching, area matching, filter based) are being applied to compensate the INS error (Titterton and Weston, 2004; Groves, 2013). However, the divergence of position sometimes occurs in the filter based algorithm when the linearity between measurements and states is not preserved (Perea *et al*., 2007). Also, most navigation algorithms generate less precise navigation results if the local signatures of geophysical data are not significantly dominant (Groves, 2013; Lee *et al*., 2013). Since not only characteristics of the geophysical data but the strengths and weaknesses of each navigation algorithm are different, a new type of study which combines various geophysical data or algorithm is getting started to conserve stability of the navigation performance (Robins, 1998; Liu *et al*., 2009; Xiong *et al*., 2013; Lee *et al*., 2014).

Received 2016. 07. 21, Revised 2016. 08. 04, Accepted 2016. 08. 17
1) Member, Dept. of Geoinformatics, University of Seoul (E-mail : leejs@uos.ac.kr)
2) Corresponding Author, Member, Dept. of Geoinformatics, University of Seoul (E-mail : jkwon@uos.ac.kr)

From the same point of view, the performance of GGRN constructed based on an EKF (Extended Kalman Filter) was analyzed and the necessity of the combination of gravity gradient with terrain or filter based algorithm with the profile matching algorithm was suggested as a way to support more stable and precise navigation (Lee *et al*., 2014; Lee and Kwon, 2014). In this study, therefore, a new type of combination navigation algorithm which uses both gravity gradient and terrain DB, as well as EKF and profile matching algorithm, was developed. The performance and its effectiveness were evaluated by comparing with each GGRN, TRN, and profile matching results.

2. Methodologies

In general, each geophysical data show different characteristics despite the same region. Also, the resolution and precision of the constructed geophysical DB are not identical. Therefore, GGRN sometimes generates better navigation results than TRN, but sometimes does not. Also, the profile matching algorithm which stacks obtained information and compares it with DB would be more stable than a filter based algorithm when geophysical data varies significantly. It is because a filter based algorithm sometimes causes wrong or over-correction when linearity between measurements and states is not guaranteed. In this kind of situation, a combination of various geophysical DBs or algorithms would be implemented to complement pros and cons of each geophysical DB and navigation algorithm. In this study, the EKF based algorithm developed in the previous study was modified to apply both gravity gradient and terrain data as measurements, and the profile matching algorithm which uses terrain data was constructed. Then, the final navigation position of the vehicle was determined by combining the result from EKF with one from the profile matching algorithm.

Fig. 1 illustrates the principle of the combined navigation algorithm which uses heterogeneous geophysical DBs and algorithms. The position and attitude error of the INS are compensated based on gravity gradient and terrain DB using EKF algorithm every epoch. Also, a measured terrain information is stored as a form of a profile. If vehicle obtains enough terrain information or a specific condition is met, candidate profiles are extracted from the DB and compared to the obtained profile. When a profile is selected, there are two candidate positions (one from the EKF and the other from the profile matching algorithm) at the same epoch. Therefore, it is possible to check the reliability of the filter based position and re-determine the final position of the current epoch by combining them.

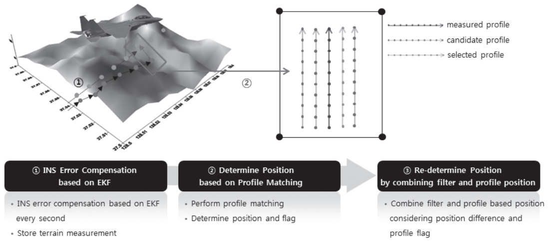

Fig. 1. Principles for combining heterogeneous geophysical DBs and algorithms

2.1 Combination of geophysical DBs using EKF

The geophysical DB referenced navigation algorithm is categorized according to the way to apply obtained geophysical information. The batch process stacks obtained geophysical information for a certain period of time and compares it with DB. On the other hand, the sequential process which uses a various filter (e.g. EKF, UKF (Unscented Kalman Filter), BKF (Bank of Kalman Filter), etc.) estimates the unknowns or their errors based on the relation between measurements and unknown parameters. Among various filters, EKF is broadly applied due to effectiveness regarding the calculation time (Haykin, 2001). Therefore, Lee *et al*. (2014) realized GGRN and TRN based on the EKF and analyzed their performance considering various factors such as DB-sensor error, DB resolution, update rates. In the simulation, it was found that TRN is relatively more stable than GGRN if the currently available geophysical sensor and DB are applied. However, TRN sometimes diverged due to non-linearity between measurements and states. Therefore, it was pointed out that the GGRN is still beneficial, and six gravity gradient components which show different local variation could be a way to complement the weakness of TRN.

In this study, the previously constructed GGRN has been modified to include terrain data. In other words, a centralized type of EKF is developed to use both gravity gradient and terrain for the navigation error compensation. In general, the centralized filter is known that it has the benefit of minimal information loss (Skog, 2009). Eq. (1) shows the measurement equation of GGTRN (Gravity Gradient and Terrain Referenced Navigation). Simply, it could be understood as a modified version of GGRN by adding one terrain difference as a measurement. The measurement vector z_k is a form of difference between information obtained from sensors and that from DB or INS and a total of nine measurements are included every epoch : six for gravity gradient, one for terrain, height and yaw, respectively. The design matrix H_k for the gravity gradient and terrain is determined as the slope of geophysical data in the latitudinal and longitudinal directions. x_k is the 15-state vector and v_k is the measurement noise vector . For a more detalied explanation on the system model and the measurement equation, please refer Lee *et al.* (2015).

$$z_k = H_k x_k + v_k,\ \ v_k \sim N(0, R) \tag{1}$$

$$\text{where }\ z_k = \begin{bmatrix} \delta\Gamma^n - \left[\frac{\partial L_\Psi^n}{\partial \Psi^n}\right]\left[\frac{\partial \Psi_{in}^n}{\partial cb_u}\right] c\delta b_u{}_{6\times1} \\ H_{DB} - (H_{baro} - H_{radar}) \\ h_{INS} - h_{baro} \\ \gamma_{compass} - \gamma_{INS} \end{bmatrix},$$

$$H_k = \begin{bmatrix} \frac{\partial \Gamma_{map}}{\partial \varphi}{}_{6\times1} & \frac{\partial \Gamma_{map}}{\partial \lambda}{}_{6\times1} & 0 & \mathbf{0}_{6\times12} \\ \frac{\partial H_{DB}}{\partial \varphi}{}_{6\times1} & \frac{\partial H_{DB}}{\partial \lambda}{}_{6\times1} & 0 & \mathbf{0}_{6\times12} \\ 0 & 0 & 1 & \mathbf{0}_{1\times12} \\ \mathbf{0}_{1\times6} & 0 & 0\ \ 1 & \mathbf{0}_{1\times6} \end{bmatrix} + \begin{bmatrix} \left[\left[\frac{\partial L_\Psi^n}{\partial \Psi^n}\right]\left[\frac{\partial \Psi_{in}^n}{\partial r^n}\right]\right]_{6\times3} & \mathbf{0}_{6\times12} \\ \mathbf{0}_{1\times15} & \\ \mathbf{0}_{1\times15} & \\ \mathbf{0}_{1\times15} & \end{bmatrix},$$

2.2 Profile matching algorithm

Because geophysical data does not vary linearly in the latitude or longitude direction and sometimes shows a relatively small variation, the filter based algorithm occasionally diverges. In this study, the profile matching algorithm was constructed to complement the weakness of the filter based algorithm and to check the reliability of the position from filter based algorithm. It is known that the profile matching algorithm generates better performance when geophysical data shows larger variation and local characteristics so that terrain DB indicating a higher precision and resolution is applied for the profile matching.

Fig. 2 shows the flow chart of the profile matching algorithm. The vehicle obtains the height of the terrain every epoch and stacks it for 10 seconds; then stored terrain information is compared to candidate profiles extracted from DB. Under the assumption that the vehicle flies straightly from south to north direction with constant speed, candidates profiles were generated as a form of the grid by moving initial point to the latitude and longitude direction five times. The interval to the latitude direction is determined by dividing total moving distance which is calculated based on the INS-indicated position into 10, and the interval to the longitude is assumed as a half of the DB resolution (1.5arcsec = 45m) to improve the reliability of profile position. The final position of the vehicle from the profile matching is selected when the MAD (Mean Absolute Difference) of height between vehicle profile and candidate profile is the minimum. Eq. (2) represents the MAD; $H_{vehicle}$ and $H_{candidate}$ are the height of vehicle profile and candidate profile, respectively.

$$\text{MAD} = \frac{\sum_{i=1}^{10} |H_{vehicle} - H_{candidate}|}{10} \tag{2}$$

Also, Some previous studies suggested indexes (e.g. σ_T, σ_Z) which show roughness of the profile for the purpose of checking the feature of the terrain and concluded that the performance of the profile matching algorithm would be better when those indexes are large (Siouris, 2004). In this study, both indexes are adopted; σ_T which represents the overall variation of heights and σ_Z which means the variation of the height difference are calculated using Eq. (3).

$$\sigma_T = \frac{\sum_{i=1}^{10} |H_{vehicle} - \overline{H}_{vehicle}|}{9}, \quad \sigma_Z = \frac{\sum_{i=1}^{9} \left|H'_{vehicle} - \overline{H'}_{vehicle}\right|}{8},\ \ H' = H_{i+1} - H_i \tag{3}$$

where H is the height of a vehicle profile, H' is the height difference of a vehicle profile, $\overline{H}$ and $\overline{H'}$ are the average of height and height difference over a vehicle profile.

Because the characteristics of each profile are different, it is difficult to set certain criteria to judge whether the terrain roughness is large enough. Therefore, it was determined empirically through trial and error; σ_T and σ_Z should be larger than 40% of the standard deviation of heights of whole candidate profiles and 10m, respectively. Then, the position update is conducted when those indexes are larger than the criteria.

Although the profile shows the minimum MAD, it is risky to select it due to DB and sensor error. Therefore, uniqueness check process was considered additionally to check the reliability of the selection. In the uniqueness check, two basic steps were set to find more trustworthy position; First, a selected profile should show obviously smaller MAD than other candidates. Therefore, a similarity between a pair of candidate profiles showing minimum and second minimum MAD, and second minimum and third minimum MAD were checked. In this study, it was assumed that the profile shows the smallest MAD is surely reliable when the ratio of MADs of two profiles is smaller than 80%. The criterion, 80%, was also empirically determined based on the many tests. In the simulation, 90% was not enough to isolate the profile, and many profiles did not pass the criteria of 70%. Second, the position of selected profile which passed the first condition is verified. If the ratio of MADs is small and the position difference between two profiles is large, it could be concluded that the position is trustable. Otherwise, it makes sense the position difference should be small when the ratio is large. In this case, the position was calculated on an average of the positions of two profiles. After considering conditions above, the final position was determined together with the flag of reliability. The flag 1 and 2 show the high reliability, whereas flag 10 and 11 indicates the low reliability. Additionally, an exceptional condition (flag 5) is constrainingly added to prevent the non-correction for a long time due to small σ_T and σ_Z.

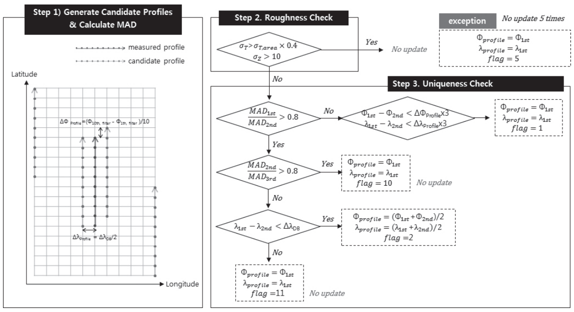

Fig. 2. Flow-chart of the profile matching algorithm

2.3 Combination of positions from filter and profile matching algorithm

The final solution from the combination of EKF and profile matching is calculated by updating the estimates from EKF with estimates from the profile matching through weight average at every 10 seconds. The weight of the solution of the EKF and the profile matching is determined considering position difference between the EKF and the profile matching, profile flag, and roughness of profile. Also, the variance for the position from the profile is assigned rather heuristically to update the P matrix of EKF to reflect the change of the position by the combination of EKF and profile matching.

When the position difference is smaller than 10m, the final position and its variance (P matrix) are determined on the average assuming the uncertainty of position from the profile is 10m.

If the position difference is larger than 45m which is the interval in the longitude direction, the profile flag and roughness of the profile are additionally considered. In case the profile flag is 1, it is assumed that the position from the profile matching is more trustworthy so that the weight of the profile and the filter is allocated to be 3 and 1, respectively. If the profile flag is 2 or 5, the weight is switched to be 1 and 3. Because position difference is smaller than 45m, the uncertainty of the profile position is supposed to be 45m. In the previous chapter, the profile matching does not update the position when the profile flag is 10 or 11. However, combining filter based position with profile solution would be a better option to bind the wrong or over-correction of the filter. Especially, the horizontal error decreases significantly when the position from filter and profile locates opposite side with respect to the INS-indicated position. Thus, condition for the profile flag 10 and 11 is added. If roughness is larger enough (σ_T is larger than 30 and σ_Z is larger than 15), the weight is assumed to be same as flag 2, but the uncertainty of profile is set to be 67.5m which is 1.5 times larger than 45m. If not, the weight is adjusted to be 5 and 1, and the uncertainty of the profile is set to be 90m.

Moreover, flag 10 and 11 frequently occur when the position difference of the latitude or longitude is larger than 45m. Thus, only the roughness of the profile is considered to allocate the weights and uncertainty. If the roughness of the profile is large, the weight is applied to be 10 and 1, and the precision of 180m is set as many epochs show more than 90m of position difference. Otherwise, the final position is determined to select the filter based position, and the P matrix of the filter is doubled to give more uncertainty to the EKF solution. Eq. (4) shows the way to determine the final position and P matrix, and the allocated weight and the precision of profile is summarized in Table 1. In the equation and table, ϕ, λ are the latitude and longitude of the vehicle, P indicates the position part of P matrix.

$$\phi_{new} = (W_{filter} \times \phi_{filter} + W_{profile} \times \phi_{profile})/(W_{filter} + W_{profile})$$

$$\lambda_{new} = (W_{filter} \times \lambda_{filter} + W_{profile} \times \lambda_{profile})/(W_{filter} + W_{profile}) \quad (4)$$

$$P_{new} = (W_{filter} \times P_{filter} + W_{profile} \times P_{profile})/(W_{filter} + W_{profile})$$

Again, there is no alternative but to allocate the weight and precision of the profile empirically due to inconsistency in geophysical data and each algorithm. Therefore, numerous simulation tests were conducted to find the most suitable values (e.g. various values such as 2, 3, 5, 10 were applied for weight; multipliers such as 1.5, 1.7, 1.8, 2 were applied to determine the P matrix). Then, the final weight and uncertainty of the profile in Table 1 were determined throughout trial and error.

3. Performance Analysis of Combining Heterogeneous DB and Algorithm

The performance of combining heterogeneous DB and algorithm is evaluated through simulation tests. In the simulation, it is supposed that the vehicle flies with navigation-grade IMU (Inertial Measurement Unit), FTG (Full Tensor Gradiometer) which obtains six gravity gradients, radar altimeter as well as six gravity gradient DBs and terrain DB. Also, a barometer and a compass are added as complementary sensors to compensate the altitude and yaw error of INS. The flight altitude and speed are 3,000m and 350km/h, respectively. The specification of DB and sensors used in the simulation is described in Table 2.

A total of nine trajectories are generated from south to north direction with a 0.25° interval from longitude 127° to 129°. Among those nine trajectories, from trajectory no. 1 to no. 7 flies from latitudes 35° to 38° but trajectory no. 8 and no. 9 flies from latitudes 35° to 37.5° to avoid the ocean area.

Table 1. The standard to combine filter based algorithm and the profile matching algorithm

<table>
<tr><th colspan="3">Condition</th><th>New Position and P matrix</th></tr>
<tr><td colspan="3">$|\phi_{filter} - \phi_{profile}| < 10m$,
$|\lambda_{filter} - \lambda_{profile}| < 10m$</td><td>$W_{filter} = 1,\ W_{profile} = 1,\ P_{profile} = 10\text{m}$</td></tr>
<tr><td rowspan="4">$|\phi_{filter} - \phi_{profile}| < 45m$,
$|\lambda_{filter} - \lambda_{profile}| < 45m$</td><td colspan="2">Profile flag = 1</td><td>$W_{filter} = 1,\ W_{profile} = 3,\ P_{profile} = 45m$</td></tr>
<tr><td colspan="2">Profile flag = 2 or 5</td><td>$W_{filter} = 3,\ W_{profile} = 1,\ P_{profile} = 45m$</td></tr>
<tr><td rowspan="2">Profile flag = 10 or 11</td><td>$\sigma_T > 30$,
$\sigma_Z > 15$</td><td>$W_{filter} = 3,\ W_{profile} = 1,\ P_{profile} = 67.5m$</td></tr>
<tr><td>Else</td><td>$W_{filter} = 5,\ W_{profile} = 1,\ P_{profile} = 90m$</td></tr>
<tr><td rowspan="2">$|\phi_{filter} - \phi_{profile}| > 45m$
or
$|\lambda_{filter} - \lambda_{profile}| > 45m$</td><td colspan="2">$\sigma_T > 30,\ \sigma_Z > 15$</td><td>$W_{filter} = 10,\ W_{profile} = 1,\ P_{profile} = 180m$</td></tr>
<tr><td colspan="2">Else</td><td>$W_{filter} = 1,\ W_{profile} = 0,\ P_{filter} = P_{filter} \times 2$</td></tr>
</table>

Table 2. Specification of DB and Sensor for GGRN and TRN

GGRN			TRN		
DB resolution [arcsec]	DB precision [Eo]	Sensor precision [Eo]	DB resolution [arcsec]	DB precision [m]	Sensor precision [m]
30	3	3	3	16	10

3.1 Combination of geophysical DBs using EKF

The effect of a combination of geophysical DBs is evaluated by comparing the results from the GGRN, TRN and GGTRN. The performance is evaluated with the standard deviation of two-dimensional position error with respect to the simulated true trajectory.

Table 3 shows the positioning errors each trajectory in the GGRN, TRN and GGTRN. In the case of GGRN, the horizontal precision appears from 53m to 193m and the average horizontal precision is about 115m. TRN shows better performance in the trajectory no. 1 to no. 7 (except trajectory no. 2) than GGRN. However, trajectory no. 8 and no. 9 which start a flight in the plain area and pass abruptly changing region do not compensate the INS error properly so that the horizontal error of the two trajectories is larger than the pure navigation solutions. It is already pointed out the weakness of TRN which originates in the use of only one terrain difference as a measurement to compensate the horizontal position error of INS. Therefore, it is difficult to conclude that TRN shows better performance than GGRN although the average of TRN except the two trajectories is about 54m. The last column in Table 3 shows the navigation results from GGTRN which use both gravity gradient and terrain DB. Many trajectories (except the trajectory no. 8 and 9) show improved results. It should be noted that those two trajectory shows divergence in TRN and adding gravity gradient does not improve the divergence in positioning. The average horizontal error except the diverging trajectories is about 21m.

The largest improvement due to a combination of geophysical DBs is shown in trajectory no. 2. The horizontal error of GGRN and TRN are about 193m and 295m, but the horizontal error decreased to 22.630m in GGTRN. It is found that the navigation error of both GGRN and TRN is getting larger in the starting zone and after 1800 seconds of flight, respectively (Fig. 3). However, the large error of GGRN in the starting zone is bound by the and GGRN makes a positive effect on reducing horizontal error when the horizontal error of TRN increases from 1800 seconds. As a result, GGTRN shows much stable navigation performance over the whole trajectory.

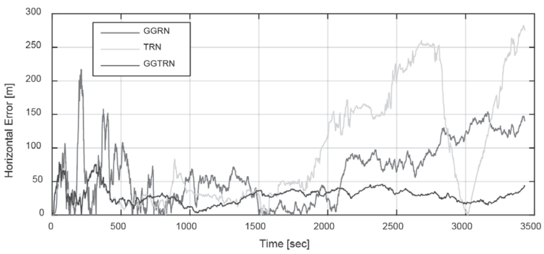

Fig. 3. Horizontal error from GGRN, TRN and GGTRN in the trajectory no. 2

Table 3. Navigation results of filter based algorithm (GGRN, TRN, GGTRN)

Traj. no.	GGRN	TRN	GGTRN	Traj. no.	GGRN	TRN	GGTRN
1	192.337	22.821	63.714	6	71.020	15.058	16.310
2	192.678	294.579	22.630	7	87.817	16.227	13.321
3	52.727	11.092	10.985	8	141.560	36976.350	4472.651
4	41.972	9.577	9.847	9	64.557	8272.175	1004.115
5	187.572	7.199	8.644	average	114.693	53.793*	20.779*

* means the average of horizontal error when trajectory showing divergence is excluded

Of course, not all trajectories generate better navigation results in GGTRN. Among nine trajectories, only three trajectories show more precise results. However, it should be mentioned that the magnitude of degradation is not that big. Moreover, the horizontal position error decreases significantly compared to results from GGRN. Therefore, it could be stated that the combination of geophysical DBs makes a positive effect on the navigation results.

3.2 Profile matching algorithm

The results from the profile matching are summarized in Table 4. The horizontal error of the profile matching distributes from 40m to 106m, and its average is about 67m. While the results from the filter based algorithm show some inconsistent performance in each trajectory, the profile matching generally shows much consistent positioning results with no divergence.

The possibility of the complement of different navigation algorithms can be seen in Fig. 4. After starting a flight, the horizontal error increases in the time window between 300 seconds and 500 seconds when vehicle flies above smoothly changing area. Also, those navigation errors get larger from 800 seconds in the abruptly changing area due to lack of linearity between measurement and states. Therefore, the overall navigation error of TRN and GGTRN in the trajectory no. 8 is calculated larger than 1km. However, this kind of irregular variation in the terrain DB could be feature points for bounding navigation error positively in the profile matching algorithm. The horizontal error in the profile matching increased from 800 seconds to 1800 seconds, but the maximum error is bound to the few hundred meters. Accordingly, the overall navigation performance is determined as 100m level.

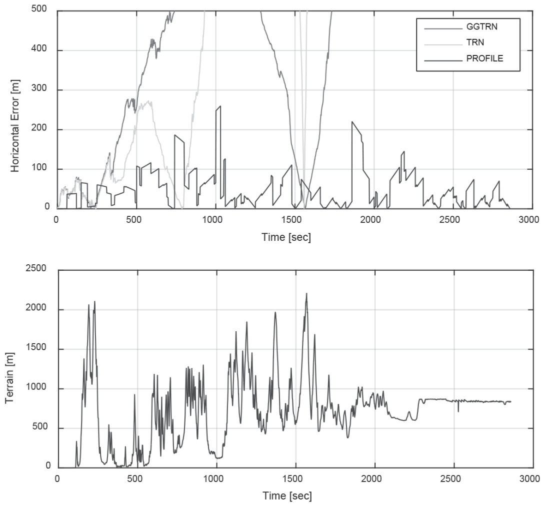

Fig. 4. Horizontal error and the terrain of the trajectory no. 8

3.3 Combination of positions from filter and profile matching algorithm

As the last step, GGTRN and the profile matching algorithm have been combined, and its performance is compared to the best result for each trajectory from all filter based and the profile matching algorithm (Table 5). In Table 5, a trajectory which shows better performance through a combination of geophysical data and the algorithm is marked with *, and performance ratio is calculated by dividing the navigation result from a combination algorithm with the one showing the most stable results among GGRN, TRN, GGTRN, and the profile matching. The average of horizontal error over whole trajectories, 17.9m, is the most precise one compared to the filter based algorithms and the profile matching. Of course, not all trajectories generate improved navigation results; a total number of four trajectories show better performance. Although

Table 4. Navigation results of the profile matching algorithm

Traj. no.	1	2	3	4	5
Horizontal error [m]	66.438	90.555	65.529	49.100	40.391
Traj. no.	6	7	8	9	average
Horizontal error [m]	47.718	50.077	106.079	89.316	67.245

Table 5. Navigation results of a combination of GGTRN with the profile matching

Traj. no.	Horizontal error [m]	Performance Ratio [%]	Traj. no.	Horizontal error [m]	Performance Ratio [%]
1*	17.946	127.165	6	16.625	90.574
2*	22.567	100.279	7	22.496	59.215
3	16.774	65.488	8*	17.932	591.563
4	14.105	67.898	9*	19.696	327.767
5	12.826	56.128	Average	17.885	

* indicates the trajectory which shows better performance

other five trajectories do not show a large improvement compared to GGRN, TRN or GGTRN, however, the strength of the final combination algorithm should be emphasized regarding stability. As shown in Table 5, the results from the final combination algorithm have a range of 14-23m of horizontal precision, and there is not a large difference in the performance among trajectories. In addition, no divergence occurs. It should be reminded that the P matrix was tuned considering the potential precision of the profile matching. When only the position is re-determined without tuning the P matrix, the average of horizontal error is about 28.610m. Judging from the simulation tests, tuning of P matrix seems to guarantee more stable navigation results in a combination of algorithms, although the magnitude and the weights are determined empirically.

To examine the advantage of a combination of geophysical data and algorithm, the horizontal results in two trajectories, trajectory 8 showing divergence in GGTRN and trajectory 5 showing poorer results in a combination algorithm, are plotted in Fig. 5. As already found before, navigation results from GGTRN diverge from 300 seconds in trajectory no. 8 due to the non-linearity problem. However, the horizontal error is bound by combining the profile matching solution with GGTRN so that overall stable navigation results are obtained.

In contrast, trajectory no. 5 shows the best performance in the TRN, as 7.199m. When combining TRN with gravity gradient or GGTRN with the profile matching, the horizontal error is degraded to the 8.644m and 12.826m, respectively. It is because GGRN and the profile matching algorithm have a relatively larger horizontal error than TRN, as shown in the

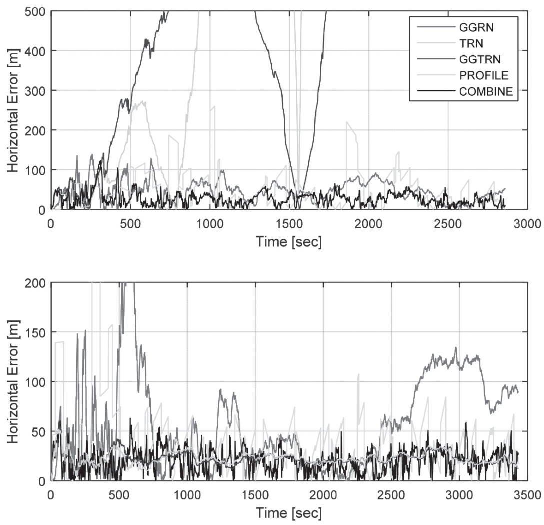

Fig. 5. Horizontal error of each navigation algorithm (Up: trajectory no.8, Bottom: trajectory no.5)

figure. However, about 188m of horizontal error of GGRN and 40m error of the profile matching decreases significantly, and 13m of horizontal error in a combination algorithm is not that large. Therefore, it could be stated that the combination algorithm guarantees the stability.

4. Conclusions

To complement the weakness of filter based algorithm using sole geophysical DB, a new type of algorithm which combines heterogeneous geophysical DBs and algorithms was suggested, and its performance was evaluated. Filter based algorithm was modified to use both gravity gradient and terrain data at the same time, and the profile matching algorithm which finds a position of the vehicle by comparing stored terrain information with DB was constructed. Then, the final position of the vehicle was determined on the basis of a combination of two positions from filter based and the profile matching algorithm considering its reliability and the local roughness.

The simulation results show that GGTRN which uses gravity gradient and terrain generally generates more stable navigation results than GGRN or TRN. Especially, the performance in one trajectory which shows 192.7m and 294.6m of error in GGRN and TRN is improved to 22.6m.

In the case of the profile matching algorithm, the local terrain roughness and the uniqueness of trajectories were checked to find the most reliable trajectory. In the simulation, the average of horizontal error over the whole trajectories is calculated as 67.2m and the two trajectories which diverge on the filter based algorithm are successfully bound to the 100m level.

When combining GGTRN with the profile matching algorithm, the average of horizontal error is calculated as 17.9m. It is the most stable navigation result compared to those from other algorithms(e.g. GGRN, TRN, GGTRN and the profile matching algorithm) constructed in this study. Also, no divergence occurs over whole trajectories. Especially, two trajectories which show poorer navigation results than pure INS in the filter based algorithm show about a 20m level of precision and it is also better than the results from the profile matching. However, the improvement of performance does not occur in all trajectories; five trajectories generate better navigation results in TRN or GGTRN. Therefore, investigations on other methodologies such as combining geophysical data as a form of decentralized filter or selecting more reliable position from different algorithm could be studied in the future.

Acknowledgment

This work was supported by the 2015 sabbatical year research grant of the University of Seoul

References

Cowie, M., Wilkinson, N., and Powlesland, R. (2008), Latest developments of the TERPROM® digital terrain system (DTS), *Proceedings of IEEE/ION PLANS 2008*, ION, 6-8 May, Monterey, CA, USA, pp. 1219-1229.

DeGregoria, A. (2010), *Gravity Gradiometry and Map Matching: An Aid to Aircraft Inertial Navigation Systems*, Master's thesis, Graduate School of Engineering and Management, Air Force Institute of Technology, Wright-Patterson AFB, OH, USA, 130p.

Groves, P.D. (2013), *Principles of GNSS, Inertial, and Multisensor Integrated Navigation Systems*, Artech house, Boston, MA, USA.

Haykin, S.S. (2001), *Kalman Filtering and Neural Networks*, Wiley, New York, N.Y., USA.

Hollowell, J. (1990), HELI/SITAN: a terrain referenced navigation algorithm for helicopter, *Proceedings of IEEE/ION PLANS 1990*, ION, 20-23 March, Las Vegas, NV, USA, pp. 616-625.

Laur, T.M. and Llanso, S.L. (1995), *Encyclopedia of Modern U.S. Military Weapons*, The Army Times Publishing Company with Berkley Publishing Group, New York, N.Y., USA.

Lee, D., Kim, Y., and Bang, H. (2013), Vision-based terrain referenced navigation for unmanned aerial vehicles using homography relationship, *Journal of Intelligent & Robotic Systems*, Vol. 69, No. 1, pp. 489-497.

Lee, J. and Kwon, J.H. (2014), Performance analysis of a gravity gradient referenced navigation system, *Journal of the Korean Society of Surveying, Geodesy, Photogrammetry and Cartography*, Vol. 32, No. 3, pp. 271-279.

Lee, J., Kwon, J.H., and Yu, M. (2014), Development of gravity gradient referenced navigation and its horizontal accuracy analysis, *Journal of the Korean Society of Surveying, Geodesy, Photogrammetry and Cartography*, Vol. 32, No. 1, pp. 63-73. (in Korean with English abstract)

Lee, J., Kwon, J.H., and Yu, M. (2015), Performance evaluation and requirements assessment for gravity gradient referenced navigation, *Sensors*, Vol. 15, No. 7, pp. 16833-16847.

Lee, W., Yoo, Y.M., Yun, S., and Park, C.G. (2014), Weighting logic design of hybrid database referenced navigation algorithm using multiple geophysical information, *Proceedings of 19th IFAC World Congress*, IFAC, 24-29 August, Cape Town, South Africa, Vol. 47, No. 3, pp. 3407-3412.

Liu, F., Qian, D., Liu, F., and Li, Y. (2009), Integrated navigation system based on correlation between gravity gradient and terrain, *Proceedings of International Joint Conference on Computational Sciences and Optimization*, IEEE, 24-26 April, Hainan, China, Vol. 2, pp. 289-293.

Liu, F., Qian, D., Zhang, Y., and Li, Y. (2010), A computer simulation of the influence of GGI and inertial sensors on gravity gradient aided navigation, *Proceedings of 2010 International Symposium on Systems and Control in Aeronautics and Astronautics*, ISSCAA, 8-10 June, Harbin, China, pp. 793-797.

Perea, L., How, J., Breger, L., and Elosegui, P. (2007), Nonlinearity in sensor fusion: divergence issues in EKF, modified truncated SOF, and UKF, *Proceedings of AIAA Guidance, Navigation and Control Conference and Exhibit*, AIAA, 20-23 August, Hilton Head, S.C., USA, Vol. 6514.

Richeson, J.A. (2008), *Gravity Gradiometer Aided Inertial Navigation within Non-GNSS Environments*, Ph. D. dissertation, University of Maryland, College Park, MD, USA, 405p.

Robins, A. (1998), Recent developments in the 'TERPROM' integrated navigation system, *Proceedings of the ION 44th Annual Meeting*, ION, 21-23 June, Annapolis, MD, USA, pp. 58-66.

Rogers, M.M. (2009), *An Investigation into the Feasibility of Using a Modern Gravity Gradient Instrument for Passive Aircraft Navigation and Terrain Avoidance*, Master's thesis, Graduate School of Engineering and Management, Air Force Institute of Technology, Wright-Patterson AFB, OH, USA, 164p.

Siouris, G.M. (2004), *Missile Guidance and Control Systems*, Springer Science & Business Media, Berlin, Germany.

Skog, I. (2009), *Low-Cost Navigation Systems: A Study of Four Problems*, Ph.D. dissertation, KTH Royal Institute of Technology, Stockholm, Sweden, 165p.

Titterton, D. and Weston, J.L. (2004), *Strapdown Inertial Navigation Technology*, IET, Stevenage, United Kindom.

Wang, Z. and Bian, S. (2008), A local geopotential model for implementation of underwater passive navigation. *Progress in Natural Science*, Vol. 18, No. 9, pp. 1139-1145.

Xiong, L., Xiao, L.W., Dan, B.B., and Ma, J. (2013), Full tensor gravity gradient aided navigation based on nearest matching neural network, *Proceedings of Cross Strait Quad-Regional Radio Science and Wireless Technology Conference*, IEEE, 21-25 July, Chengdu, China, pp. 462-465.

Zhang, F., Chen, X., Sun, M., Yan, M., and Yang, D. (2004), Simulation study of underwater passive navigation system based on gravity gradient, *Proceedings of International Geoscience and Remote Sensing Symposium*, IEEE, 20-24 September, Anchorage, AK, USA, Vol. 5, pp. 3111-3113.